Materials Today Bio 31 (2025) 101456

Contents lists available at ScienceDirect

Materials Today Bio

journal homepage: www.journals.elsevier.com/materials-today-bio

One-step fabrication of 3D-aligned human skeletal muscle tissue and measurement of contractile force for preclinical drug testing

Azumi Yoshida [a], Kazuki Baba [b], Hironobu Takahashi [a,*], Kenichi Nagese [b,c], Tatsuya Shimizu [a]

[a] Institute of Advanced Biomedical Engineering and Science, Tokyo Women's Medical University, Tokyo, 162-8666, Japan
[b] Faculty of Pharmacy, Keio University, Tokyo, 105-8512, Japan
[c] Graduate School of Biomedical and Health Science, Hiroshima University, Hiroshima, 734-8553, Japan

ARTICLE INFO

Keywords:
Muscle tissue engineering
Human muscle tissue model
Muscle contraction
Contractile force
Muscle fatigue
Drug discovery

ABSTRACT

Human muscle tissue models are critical to understanding the complex physiology of skeletal muscle in studies of drug discovery, development, and toxicity profiling in the human body. However, due to the challenges in in vitro maturation of human muscle cells, few research groups developing their own tissue engineering techniques have succeeded in producing contractile human muscle tissues. Moreover, a more sophisticated method is necessary to measure contractile forces generated by the muscle tissues for preclinical studies in muscle physiology and drug discovery. Although a few research groups have established their own tissue model systems that measure contractile force, they require multi-step fabrication processes to produce human muscle tissues sufficiently functional to be able to measure the contractile forces. To improve the usability of our tissue model system, this study focused on simplifying the tissue engineering approach to produce a practical muscle tissue model.

In this study, muscle satellite cells were simply mixed with a combination of fibrinogen, thrombin, and Matrigel before gel formation. The presence of muscle satellite cells induces gel compaction and spontaneously induces unidirectional stretching of the gel, resulting in the muscle satellite cells being aligned three-dimensionally with the direction of stretching. Furthermore, this gel environment promotes the maturation of the human muscle progenitor cells into aligned myofibers, also provides the tissue with an elastic platform for muscle contraction, and allows the attachment of the muscle tissue to a device for measurement of contractile force. Therefore, this one-step tissue fabrication allowed us to produce 3D-aligned human muscle tissues and this tissue model is ready to use for the measurement of contractile forces. In fact, the muscle contractions created by electrical and chemical stimulation were quantitatively determined using our measurement system. In addition, the impact of some representative drugs on this muscle tissue were able to be monitored in real-time throughout the changes in contractile forces.

In conclusion, our tissue model system, produced by a simple fabrication method, can be used for preclinical in vitro studies in muscle physiology and drug discovery.

1. Introduction

Traditionally, small animal models have been used for drug discovery, development, and toxicity profiling in preclinical studies. However, only 10 % of drugs that pass preclinical animal tests become clinically approved due to unexpected drug toxicity or insufficient therapeutic benefits [1,2]. This is mainly because of the critical gaps in drug response and toxicity between animals and humans [3,4]. Since animal models have limitations in understanding mechanisms in the human body, human cell-based tissue models have many significant advantages for use in preclinical drug testing [5–9]. In studies of muscle diseases, human muscle tissue models promise a better understanding of disease mechanisms and facilitate the discovery of new drugs [10–13]. In addition, the high metabolism of skeletal muscle results in a greater

This article is part of a special issue entitled: Surface & Interface published in Materials Today Bio.

* Corresponding author.
E-mail address: takahashi.hironobu@twmu.ac.jp (H. Takahashi).

https://doi.org/10.1016/j.mtbio.2025.101456
Received 12 July 2024; Received in revised form 18 December 2024; Accepted 3 January 2025
Available online 11 January 2025

exposure of administered drugs to the tissue, and often results in severe unexpected effects on muscles [3,14,15]. Therefore, muscle tissue models are also required when studying drug toxicology [16,17]. Tissue engineering technologies have allowed us to engineer muscle tissues from cultured muscle progenitor cells in vitro. Due to the difficulty in stimulating the maturation of human muscle cells, a number of research groups have reported on the modeling of muscle tissues using rodent muscle progenitor cells [18–20]. However, a large number of drug development trials have not been able to determine the pathogenic mechanism in human cells because of the limitations of animal tissue models. Given the critical gaps between humans and animals, it is important to use human cell-based muscle tissues in preclinical applications.

Native skeletal muscle has a highly oriented structure of parallel bundles of contractile myofibers. Although in the last few decades, several research groups have reported strategies to replicate the unique aligned structure of native muscle, only a few groups have succeeded in the production of human cell-based muscle tissue with biomimetic structures and functions [16,21–25]. In some previous studies, the tissue formation technique stimulates the formation of 3D-aligned structures simply by mixing muscle cells with extracellular matrix (ECM) proteins. Even though the miniaturized structures of these tissue models have potential to be used for drug screening, the contraction displacement still needs to be analyzed using a motion analysis tool to determine functionality of the muscle tissues. On the other hand, we demonstrated that our tissue model system allows us to directly measure contractile force generated by muscle tissues. In our previous study, we reported on our unique method for the production of human muscle tissues based on our original tissue engineering method, “cell sheet-based engineering” [23,24]. The thermoresponsive substrate we use allows confluent cells to be released from the culture surface by lowering the temperature and subsequently manipulated as a sheet-shaped assembly, a “cell sheet” [26,27]. We also were able to engineer muscle tissue having a biomimetic-aligned structure, by developing a micropattern on our thermoresponsive substrate [28,29]. Muscle cells aligned on the micropatterned substrate can be transferred as a cell sheet onto a fibrin-based gel that facilitates the functional maturation of the aligned muscle satellite cells. Based on the cell sheet-based tissue fabrication process, human muscle sheet tissues with a biomimetic-aligned structure can now be uniquely produced on the gel platform [23,24,30–32].

In addition to the production of human muscle tissues having aligned structures, the technology to measure contractile forces generated by the muscle tissues is essential for preclinical studies. Since contractile ability is the fundamental characteristic of native skeletal muscle, the functionality of engineered muscle tissues allows us to understand the impact of some drugs on the tissue model in preclinical drug testing. However, few research groups have established a system to directly measure the contractile force of engineered muscle tissues [16,21,23]. Furthermore, previous methods require complicated stepwise fabrication to meet the needs of contractile measurements. In this study, we focused on the simplification of tissue modeling to improve the usability of muscle tissue models. Muscle satellite cells were simply incorporated into the gel with an adaptor customized specifically for attaching to our measurement device. This tissue fabrication allows the cells to align and mature into myofibers to mimic the structure and function of native skeletal muscle in one step. In addition, the contractile force generated by the tissue was measured by attaching to the device after functional maturation. In summary, the muscle tissues produced in this study showed great potential for use as a preclinical tissue model in studies of muscle physiology and drug screening.

2. Materials and methods

2.1. Proliferation culture of human skeletal muscle satellite cells

Human skeletal muscle satellite cells (HSkMC; Lifeline Cell Technology, Frederick, MD, USA) were used in this study. Cells were seeded in φ100 mm-culture dishes at a density of 5000 cells/cm^2 and cultured at 37 °C in a 5 % CO_2 environment. The day after seeding and every 1–2 days thereafter, the culture medium was changed until approximately 80 % confluent. The cells were passaged repeatedly to collect a sufficient number of cells for tissue fabrication [24,32]. Stem-Life Sk Medium Complete Kit (Lifeline Cell Technology) was used as the medium for cell proliferation.

2.2. Fabrication of 3D-aligned muscle tissue in one step

Fabrication of 3D-aligned muscle tissue was performed by mixing the muscle cells with fibrin-based gel. First, 3×10^6 cells harvested from culture dishes by trypsinization were suspended in 250 μL of 10 mg/mL fibrinogen from bovine plasma (Sigma-Aldrich, St. Louis, MO, USA). One mL of 4 mM calcium chloride, 500 μL of 10 U/mL thrombin from bovine plasma (Sigma-Aldrich), and 500 μL of Matrigel (Corning, NY, USA) were mixed in a φ35 mm-culture dish. Then, 250 μL of this mixture was added to 250 μL of the cell-suspended fibrinogen solution. After mixing by pipetting, the solution was poured into the gel preparation apparatus. The solution containing the cells was capped before gelation to seal the mold, and incubated for 20 min at 37 °C in a 5 % CO_2 environment. After gelation, the gels were transferred to 6-well culture plates. The growth medium was supplemented with gel lysis inhibitors, 500 KIU/mL aprotinin (FUJIFILM Wako Pure Chemical, Osaka, Japan), and 2 mg/mL 6-aminocaproic acid (ACA; FUJIFILM Wako Pure Chemical), then placed in each well and the muscle tissues were incubated in the medium at 37 °C in a 5 % CO_2 environment. After 4 days of the incubation without changing the medium, the medium was replaced with differentiation induction medium [Dulbecco’s Modified Eagle Medium (DMEM; FUJIFILM Wako Pure Chemical) supplemented with 2 % horse serum (HS; Thermo Fisher Scientific, USA), the gel lysis inhibitors, 10 μM SB431542 (Santa Cruz Biotechnology, Dallas, TX, USA) and penicillin-streptomycin] and the muscle tissues were further cultured for 7 days with medium. The medium was changed every 2–3 days. Following the differentiation induction, electrical pulse stimulation (EPS) (voltage: 10 V, frequency: 1 Hz, duration: 10 ms) using an electrical pulse generator (IonOptix, Milton, MA, USA) with carbon electrodes for 6-well plates (C-Dish; IonOptix) was continuously applied for 60 min and pauses of 180 min. This procedure (exercise for 1 h and rest for 3 h) was repeatedly performed for 1–2 days [23,24,30,31].

For microscopic observation of contraction behavior, muscle tissues were electrically stimulated (voltage: 10 V, frequency: 1 Hz or 15 Hz, duration: 10 ms) and muscle contractions induced by EPS were monitored sequentially using a phase contrast microscope equipped with a CCD camera (Basler Ace, Basler AG, Germany; 30 frames/s).

2.3. Immunofluorescence staining

Muscle tissues were fixed overnight at 4 °C in 2 % paraformaldehyde in phosphate buffered saline (PBS). The fixed samples were incubated with a blocking solution [5 % bovine serum albumin (BSA), 0.2 % Triton-X 100] (Sigma-Aldrich) for 12 h at room temperature (RT). Primary antibodies [sarcomeric α-actinin (1:500) (Abcam, Cambridge, MA, USA), myosin heavy chain (MHC) (1:200) (R&D Systems, Minneapolis, MN, USA)] were added dropwise and left at 4 °C overnight. After washing with PBS, the fixed tissues were incubated with fluorescent-labeled secondary antibody (1:1000) (Thermo Fisher Scientific) for 2 h at RT. For nuclear staining, Hoechst 33258 (Dojindo Laboratories, Kumamoto, Japan) was used and allowed to stand at RT for 1 h, then washed three times with PBS. Images were acquired with a confocal microscope FV1200 and analyzed with FV10-ASW.

To observe the cross-sectional structure of the muscle tissues, they were embedded in paraffin and sections of the muscle tissues were prepared. The sectioned specimens were soaked in xylene and ethanol. After washing twice with PBS, cells were immersed in Target Retrieval

Solution (Agilent Technologies, Santa Clara, CA, USA) and treated with antigen activation in a pressurized chamber ((1) 125 °C for 30 s, (2) 90 °C for 10 s). After the samples were brought to RT and washed three times with PBS containing 0.1 % Tween 20 (Bio-Rad Laboratories, Hercules, CA, USA) (PBST), Blocking One-Hist (Nacalai Tesque, Kyoto, Japan) was added dropwise and the samples were incubated for 1 h at RT. Primary antibodies [laminin (1:500) (Abcam), MHC (1:200) (R&D Systems), dystrophin (1:500) (Abcam)] were then added dropwise to the samples and the samples were incubated overnight at 4 °C. Following three washes with PBST, the samples were treated with the secondary antibody for 1 h at RT. The samples were washed three times with PBST followed by one wash with PBS. Finally, the samples were enclosed in ProLong Gold Antifade Mountant with DAPI (Thermo Fisher Scientific). Images were acquired with a confocal microscope FV1200 and analyzed with FV10-ASW.

2.4. Contractile force measurement of 3D-aligned muscle tissue

The contractile force measurement device was originally developed by our group, and partly customized by NIHON KOHDEN Corporation (Tokyo, Japan) [33]. The device consisted of a load cell (LVS-10GA; Kyowa Denshi Kogyo, Tokyo, Japan) and a culture bath made of acrylic plates. The load cell height is adjustable with a single-axis stage (Chuo Precision Industrial, Tokyo, Japan). The fibrin gel was suspended from the sensor rod of the load cell using an adapter. The muscle tissue was incubated in Medium 199 (Thermo Fisher Scientific) containing 2 % HS, 2 mg/mL ACA, and penicillin-streptomycin on a heating plate set at 37 °C. The medium was gently agitated during the measurement. The load cell was connected to a strain amplifier (DPM-712B; Kyowa Denshi Kogyo), and the contractile force was recorded on a PC through an A/D converter (DC-300H; NIHON KOHDEN). After the base of contraction waveform was stabilized, the contractile forces of the muscle tissues were measured by applying EPS [voltage: 35 V, frequency: 1.5 Hz (for twitch), 15 Hz (for tetanus), duration time: 10 ms] using an electrical stimulation device (SEN-3401; NIHON KOHDEN). The contractile force profiles were analyzed with LabChart 8 (AD Instruments). To optimize the contractile force measurement conditions, EPS was applied at different voltages (10, 20, 30, 35, 40, and 50 V), and contractile forces generated by the same tissue were compared. To optimize the concentration of SB431542, the muscle tissues were cultured for 7 days in differentiation induction medium supplemented at different concentrations (0, 5, 10, 25, and 50 μM). The contractile forces produced by the muscle tissues were compared to determine the effect of SB431542 on the maturation of the muscle tissues.

2.5. Drug efficacy evaluation of 3D-aligned muscle tissue

Chemically induced tissue contractility was confirmed by adding 100 mM acetylcholine chloride solution (final concentration: 1 mM) (Sigma-Aldrich) to the medium [13,16]. In the drug efficacy evaluation, two representative agents affecting ryanodine receptors, ryanodine (Santa Cruz Biotechnology) and dantrolene (Sigma-Aldrich) were used [24]. Ryanodine was added to the medium at final concentrations of 0.5, 1, and 5 μM. Dantrolene was added to the medium at final concentrations of 12.5, 25, and 50 μM. To observe changes in contractility, EPS (frequency: 1.5 Hz, voltage: 35 V, duration: 10 ms) was applied immediately after the additions of each of these agents. To determine the changes in contractile forces, the average contractile force of five twitches was calculated every minute after each addition. In addition, tetanus contractions at 0 min and 10 min were also compared. Clenbuterol (Sigma-Aldrich) was also added to the medium (final concentration: 0.1, 10, 50, and 100 μM) [24]. The EPS (frequency: 1.5 Hz, voltage: 35 V, duration: 10 ms) was applied immediately after the addition of clenbuterol to observe changes in contractility. The average contractile force of five twitches was calculated every minute after the addition of clenbuterol for 20 min. To determine the effect of clenbuterol on the ability to maintain a tetanus contraction, the gradient of a tetanus contraction profile from the starting to ending points was calculated as the force change with clenbuterol at different concentrations (0, 0.1, and 10 μM). The force change was compared before and after the addition of clenbuterol.

2.6. Statistical analysis

Data are presented as the mean ± standard deviation. Statistical analysis of the comparison of the two groups was performed by Student's t-test (Fig. 7c). One-way ANOVA (Fig. 3c and 7a) or Welch's ANOVA (Figs. 4b, 5b and 6b) was used for multiple comparisons, and Dunnett's test (Figs. 3c, 6c and 7a), Tukey's HSD (Fig. 4d), or Games-Howell test (Figs. 4b, 5b and 6b) was used as a post-hoc test. Statistical significance was considered at $^{*}P < 0.05$, $^{**}P < 0.01$. Statistical processing was performed using R Software.

3. Results

3.1. Fabrication of 3D-aligned muscle tissue in unidirectionally stretched fibrin gel

To engineer a human muscle tissue with a biomimetically aligned structure, human skeletal muscle satellite cells were encapsulated in a fibrin-based gel simply by mixing them before gel formation. The schematic illustration of the one-step tissue fabrication is shown in Fig. 1.

Attachment to the contractile force measurement device was achieved by forming the gel with an adapter specifically designed for our measurement device (Fig. 2a) [33]. The gel was anchored at two parts of the adaptor. When the gel was released from the adaptor by cutting both sides (shown as a dotted line), the gel became smaller regardless of the presence of the encapsulated cells. However, the shrinking rate was remarkably higher in gels with cells (Fig. 2a). This indicated that the presence of the cells induced compaction of the fibrin gel. In fact, some previous studies have reported that cells mediated compaction of gel made from ECM proteins [34,35]. Subsequently, this gel compaction produced anisotropy in the culture environment for the muscle cells. When the gel was released from the adaptor after 5 days, the length of the gel reduced from 16 mm to 12 mm as indicated by arrows in Fig. 2b. This suggested that due to the anchoring with the adaptor, the gel was unidirectionally stretched (extension rate: approximately 130 %). The spontaneous stretching resulted in the formation of 3D-aligned myofibers within the anisotropic gel environment (Fig. 2c–h) [36,37]. To replicate the anisotropic environment in the gel, the fibrin-based gel was manually stretched using a stretchable chamber as shown in Supplementary Figure 1a. When the gel containing muscle cells was unidirectionally stretched to 130 % using the device, the cells cultured in the gel environment formed an aligned structure (Supplementary Figure 1b). In this study, the tissue fabrication process allowed us to produce the spontaneous stretching of the fibrin gel, which then led to the formation of the 3D-aligned myofibers in the muscle tissue.

As reported by several research groups, it is difficult to produce mature human muscle tissues in a normal 2D cell culture system. On the other hand, the culture environment of fibrin gel containing Matrigel allowed the aligned muscle cells to form sarcomere structures essential for muscle contraction (Fig. 2d and e). In addition, laminin and dystrophin were localized surrounding the aligned myofibers, suggesting the formation of native-like membrane structures (Fig. 2f–h). This biological aspect is very important for our engineered muscle tissue to perform as a biomimetic tissue model [16,23,30,31]. Taken together, this tissue fabrication method allows us to simultaneously achieve the formation of biomimetic structures, including aligned myofiber structures, sarcomere structures, and membrane-like structures.

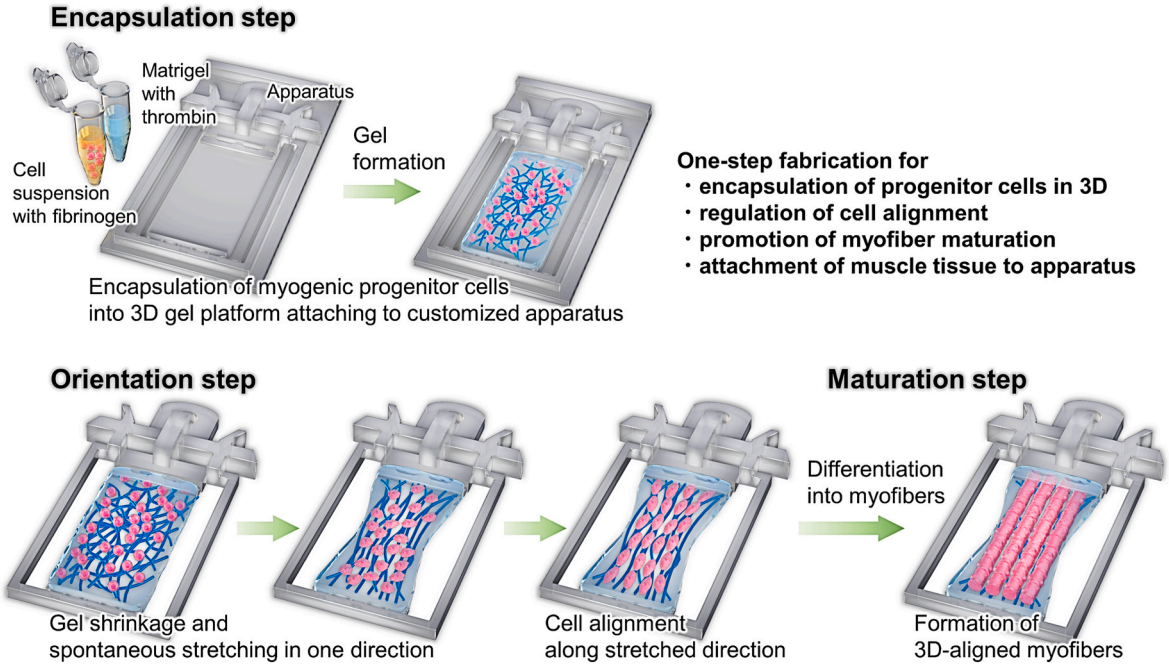

Fig. 1. Schematic illustration of the one-step fabrication of aligned muscle tissue with adaptor designed for contractile force measurement.

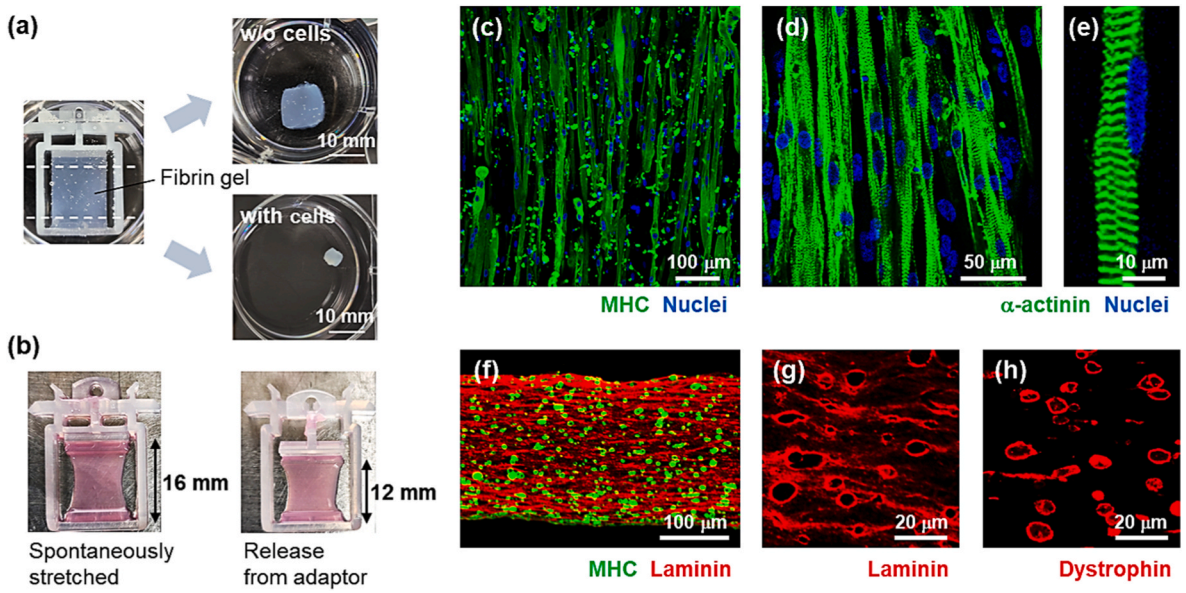

Fig. 2. One-step fabrication of a human muscle tissue composed of aligned myofibers in a fibrin-based gel adjusted for contractile force measurement. (a) A fibrin-based gel was formed with a customized adaptor to attach a contractile force measurement device, and shrunken gels, with and without cells, were released from the anchoring parts (indicated as dotted lines) by cutting both sides of the gel. (b) Fibrin-based gel with cells before and after release from the hanging adaptor. The lengths of the gel are indicated by arrows. (c–h) Fluorescence images of aligned myofibers in the gel after 7 days of differentiation induction [(c) green: MHC, blue: nuclei; (d, e) green: α-actinin, blue: nuclei; (f, g) green: MHC, red: laminin; (h) red: dystrophin]. (For interpretation of the references to colour in this figure legend, the reader is referred to the Web version of this article.)

3.2. Contractile force measurement in 3D-aligned muscle tissue

This fibrin-based gel was fabricated with a customized adaptor that allowed the muscle tissue to be lifted onto a load cell (Fig. 2a and. 3a). Importantly, the gel environment also resulted in the biomimetic-aligned structure of muscle cells and promoted maturation of the aligned myofibers (Fig. 2). Therefore, this one-step tissue fabrication allowed us to measure the contractile force generated by the functional muscle tissue just by attaching it to the device. When the muscle tissue was electrically stimulated, twitch and tetanus contractions were observed according to EPS conditions. At frequencies of 0.5 or 1 Hz, the muscle tissues produced twitch contractions (Supplementary Video 1). As the frequency increased to 5 Hz, the contractions were partially fused, and the stimulation at a frequency of 15 Hz induced a tetanus contraction (Supplementary Video 1). The tetanus contraction was dynamically shorter than the twitch contractions. Our measurement system quantitatively showed the contractile ability of the muscle tissue. The contractile forces were differentially generated according to the frequency of EPS, and the tetanus contraction produced a much higher contractile force than the twitch contractions (Fig. 3b). These contractile

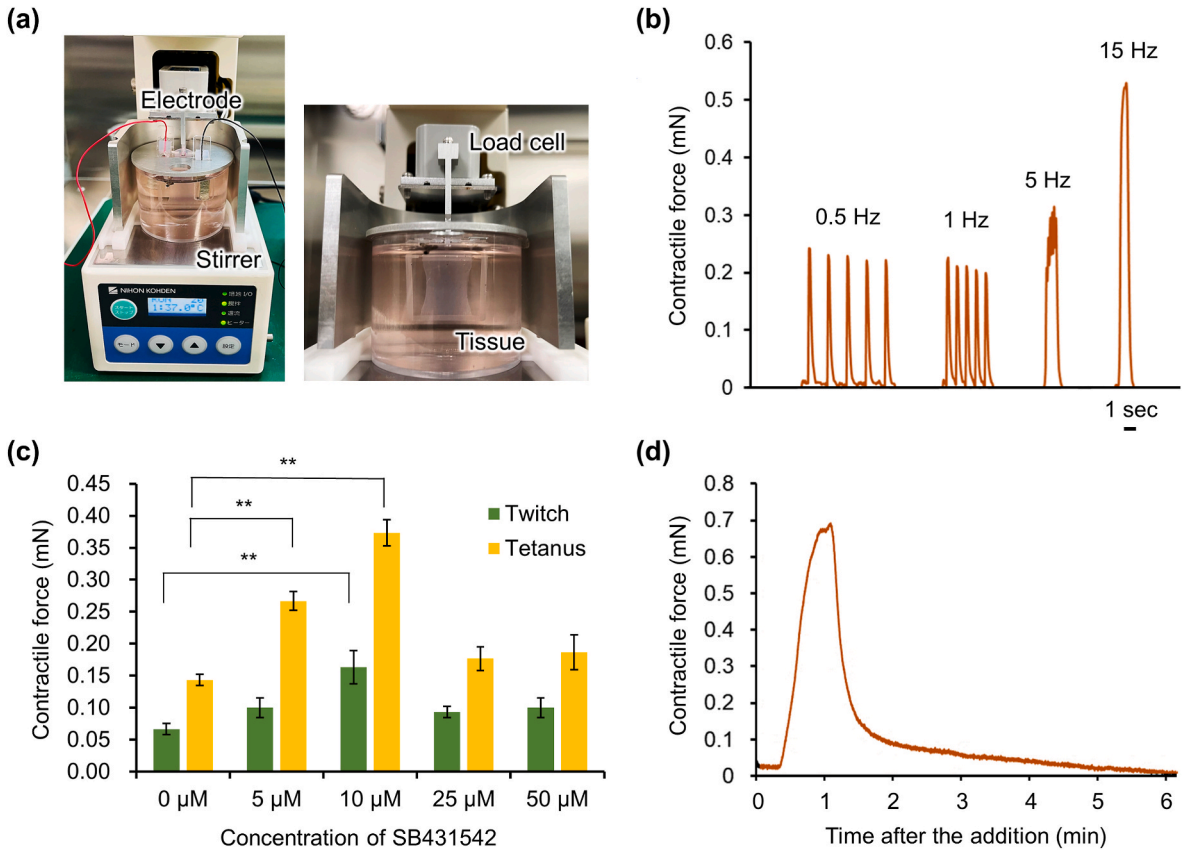

Fig. 3. Contractile force measurement of human muscle tissues stimulated electrically and chemically. (a) Photographs of muscle tissue suspended on a load cell for contractile force measurement. Two electrodes were immersed in a culture medium (phenol red free) to electrically stimulate the muscle tissue. (b) Representative profile of contractile force produced by muscle tissue at various EPS frequencies (0.5, 1, 5, and 15 Hz). (c) Contractile forces of muscle tissues generated by twitch and tetanus contractions. These tissues were cultured in a differentiation medium containing SB431542 at various concentrations (0, 5, 10, 25, or 50 μM). Contractile forces of six different tissues were measured at each concentration (n = 6). Significant differences were observed between 0 μM and 10 μM in twitch, and between 0 μM versus 5 and 10 μM in tetanus (**$P < 0.01$, Dunnett's test). (d) Representative contractile force profile of a muscle tissue chemically stimulated by the addition of ACh. (For interpretation of the references to colour in this figure legend, the reader is referred to the Web version of this article.)

behaviors shown in this study indicated that our engineered muscle tissue had physiological functions similar to native skeletal muscle. In this study, to optimize the EPS conditions, the muscle tissues were stimulated at various voltage conditions. Since the highest contractile force was measured by EPS application at 35 V (Supplementary Fig. 2), contractile forces were measured at 35 V in this study.

To enhance the differentiation of muscle cells into myofibers, muscle tissues were cultured in a medium containing 10 μM SB431542. This TGF-β1 receptor inhibitor has often been used to produce muscle tissues in vitro [38–40]. In this study, to optimize the conditions, our muscle tissues were first cultured in the medium containing SB431542 at various concentrations. The contractile force measurement allowed us to determine the effect of SB431542 on the functionality of the muscle tissues produced in this study (Fig. 3c). The effect of SB431542 was enhanced by increasing the concentration to 10 μM, resulting in generation of higher contractile forces. On the other hand, an even greater concentration of SB431542 (more than 25 μM) caused a reduction in contractile force. This may have been because the TGF-β1 receptor was excessively inhibited, which negatively influenced the maturation of the muscle tissues. From the results of the quantitative measurement, the 3D-aligned muscle tissues in this study were cultured in a medium containing 10 μM SB431542.

In native muscle, presynaptic neurons release acetylcholine (ACh) from vesicles at the axon terminals upon nerve stimulation, and the released ACh binds to acetylcholine receptor (AChR) clusters expressed on the postsynaptic myofiber membranes [41]. Similarly, when in this study the muscle tissues were chemically stimulated with ACh, they responded to chemical stimulation through AChRs. The contractile force profile indicated that the contractile behavior was different from muscle contractions induced by electrical stimulations (Fig. 3d). Through the interaction of ACh with AChRs on the myofibers, our muscle tissue gradually generated contractile force, compared with the electrically-induced contractions. This indicated that our measurement system allows us to understand various kinds of contractile behaviors quantitatively in real-time.

3.3. *Measurement of contractile force in response to drugs through interaction with ryanodine receptors*

To demonstrate the potential of our engineered muscle tissue for preclinical drug testing, changes in contractile force were measured by the addition of several pharmaceutical agents. Since it is known that ryanodine and dantrolene can influence muscle contraction through interactions with ryanodine receptors (RyRs) located in the sarcoplasmic reticulum membrane, these two drugs were used as representative agents to investigate the physiological response of the muscle tissues [42]. Since ryanodine is a well-known modulator of RyR-mediated Ca^{2+} release, it was expected that the addition of ryanodine caused a decrease in contractile force [43]. In this study, using 5.0 μM of ryanodine in the medium, the contractile forces generated by twitch contractions were remarkably decreased after 10 min of incubation (Fig. 4a). On the other hand, the additions at lower concentrations (0.5 and 1.0 μM) only caused a slight decrease in contractile force (Fig. 4b). In all cases, there was a significant decrease compared to the

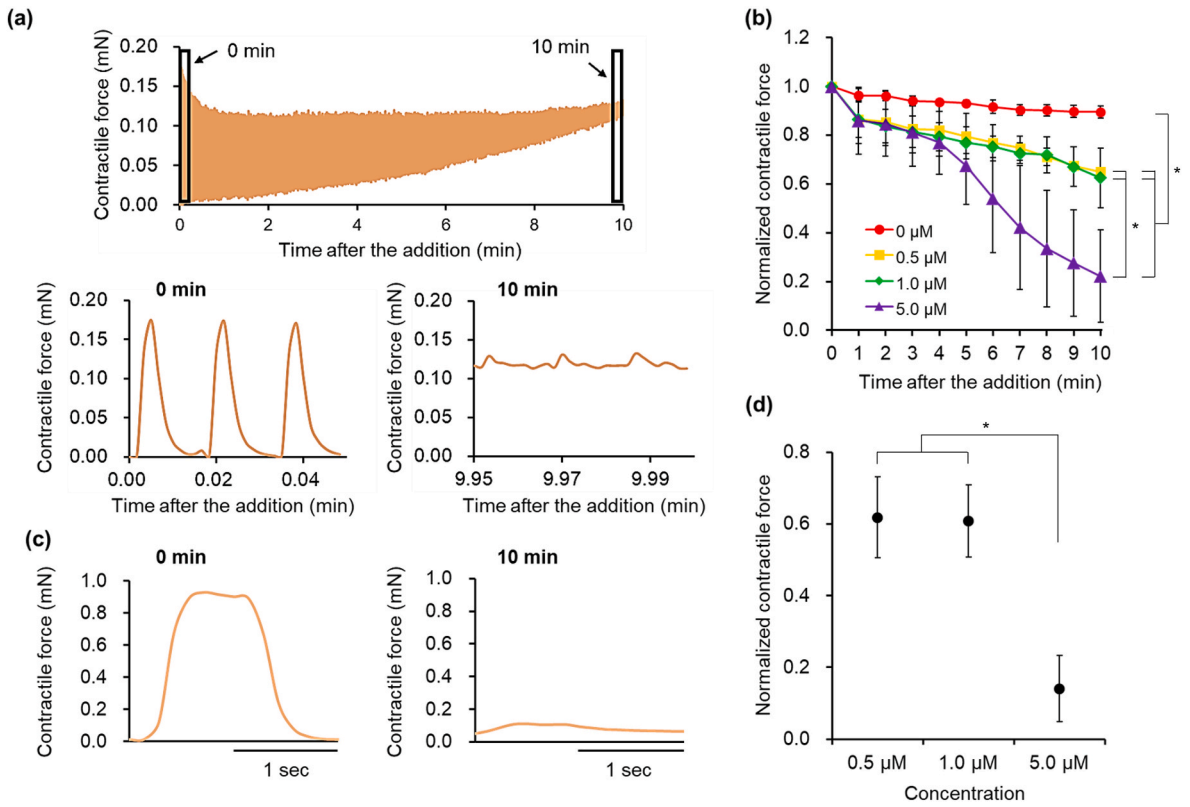

Fig. 4. Effects of ryanodine on the contractility of the engineered muscle tissue. (a) Upper: Representative profile of contractile force generated by EPS (1.5 Hz) for 10 min with ryanodine (5.0 μM). Lower: Contractile force profiles just after and 10 min after the addition of ryanodine (final concentration: 5.0 μM). (b) Change in contractile forces reduced by the addition of ryanodine at different concentrations (0.5 μM, 1.0 μM, and 5.0 μM) (n = 3). Significant differences were observed in comparison with the groups without the addition of ryanodine (0 μM), and in comparing the low (0.5 μM and 1.0 μM) and high concentration groups (5.0 μM) (*$P <$ 0.05, Games-Howell test). Contractile forces were normalized by the force at 0 min. (c) Profiles of tetanus contractions (EPS: 15 Hz) before (0 min) and after (10 min) the addition of ryanodine (final concentration: 5.0 μM). (d) Change in contractile forces of tetanus contraction by adding ryanodine at different concentrations (final concentration: 0.5 μM, 1.0 μM, and 5.0 μM). Contractile forces were normalized by the force before the addition of ryanodine (n = 3). The 5.0 μM ryanodine group was significantly lower than the other two concentration groups (*$P < 0.05$, Tukey HSD). Contractile forces shown in (b) and (d) were obtained from measurements of three different tissue samples.

group without any ryanodine. The contractile force generated by tetanus contraction was also remarkably decreased with 5.0 μM of ryanodine (Fig. 4c). On the other hand, the reduction with the lower concentrations (0.5 μM, 1.0 μM) was significantly smaller than with 5.0 μM of ryanodine (Fig. 4d). Therefore, these results indicated that the muscle tissues showed a dose-dependent change in contractile force, and our measurement system allowed us to quantitatively determine the level of dependence. In addition, we confirmed that the reduction in contractile forces was caused by the effect of ryanodine, and not by the repeated twitch contractions themselves (Supplementary Fig. 3).

The addition of dantrolene (final concentration: 50.0 μM) also caused a decrease in the contractile force of the muscle tissue (Fig. 5a). This indicated that muscle tissues physiologically respond to dantrolene, and it induced a remarkable decrease in contractile force at 10 min after the addition. Moreover, the contractile force was also significantly decreased by the addition of 25.0 μM dantrolene (Fig. 5b). However, decreasing the concentration to 12.5 μM did not significantly change the contractile force from that without the addition of dantrolene. Therefore, while the effect of dantrolene on the muscle tissue was dose-dependent, the force profile was not significantly different between the addition of 25.0 μM and 50.0 μM (Fig. 5b). Even when the concentration was increased to 100.0 μM, the contractile force was only decreased to approximately half (Supplementary Fig. 4). This limited reduction was not observed in the case of the addition of ryanodine. The same effect of dantrolene was also observed in tetanus contractions using 50.0 μM of dantrolene (Fig. 5c). However, as in the twitch contractions, the addition of dantrolene only induced a modest decrease in contractile force (Fig. 5d). Taken together, the addition of both reagents caused a decrease in contractile force through interacting with RyRs on the myofibers, but their influence on the functionality of the muscle tissues differed.

Furthermore, our tissue modeling system provided additional important information about how these two drugs influenced the contractile myofibers. The addition of ryanodine caused not only a decrease in the peak twitch contraction, but also an increase in the baseline of the profile (Fig. 4a). This indicated that the engineered muscle was unable to totally relax due to the effect of ryanodine. In fact, it is known that when ryanodine interacts with RyR, Ca^{2+} is continuously released from the sarcoplasmic reticulum, and the relaxation is partly prevented [43]. The profile of twitch contractions agreed with the known effect of ryanodine on muscle physiology. On the other hand, when dantrolene was tested on our muscle tissues, the contractile force decreased without an increase of the baseline in the profile (Fig. 5a). Dantrolene is well-known as a direct skeletal muscle relaxant that inhibits the release of Ca^{2+} from the sarcoplasmic reticulum of skeletal muscles by interaction with RyRs during excitation-contracting coupling [42,44]. Therefore, our measurement method allowed us to visualize the different responses of muscle tissues to the two drugs interacting with RyRs.

3.4. Reduction in contractile force and fatigue resistance by treatment with clenbuterol

Clenbuterol is a compound that belongs to a class of drugs called β2-agonists. This drug can cause dilation of bronchial muscles, so it is often

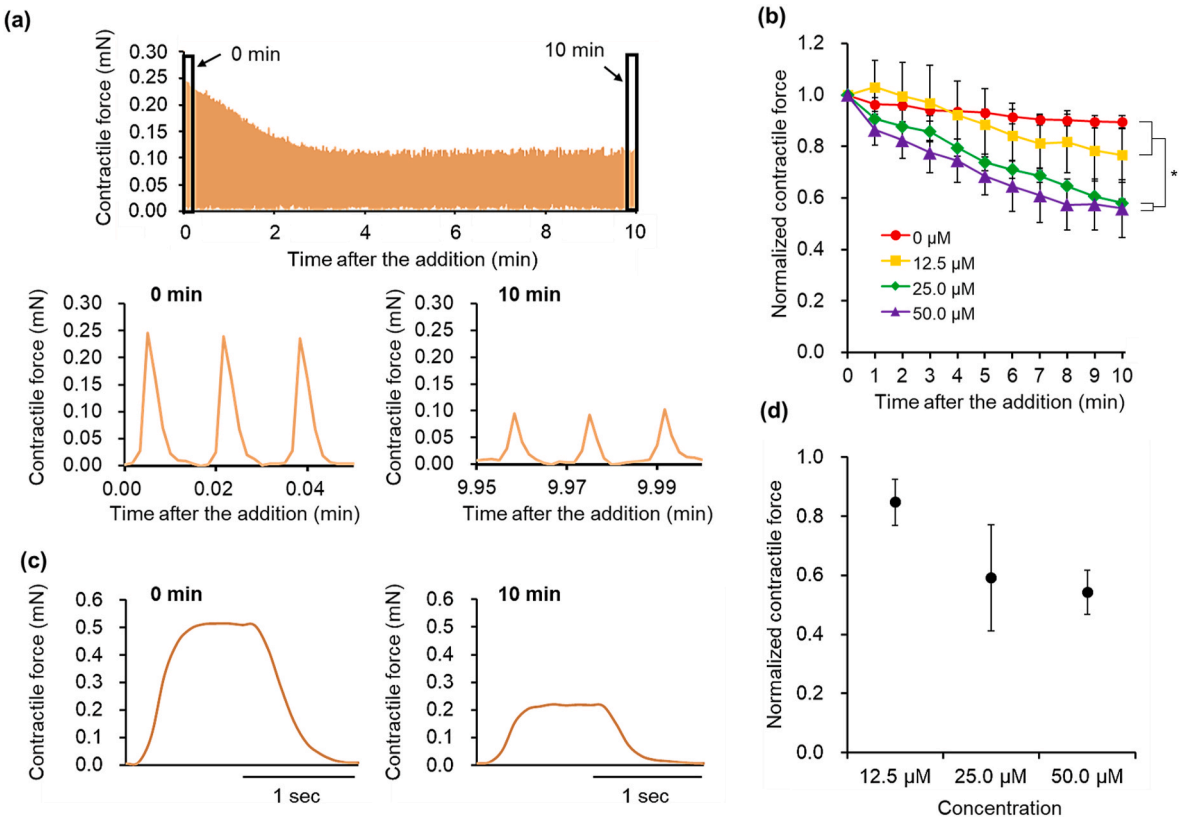

Fig. 5. Effects of dantrolene on the contractility of the engineered muscle tissue. (a) Upper: Representative profile of contractile force generated by EPS (1.5 Hz) with dantrolene (50.0 μM). Lower: Contractile force profiles in twitch contractions just after (0 min) and 10 min after the addition of dantrolene (final concentration: 50.0 μM). (b) Change in contractile forces reduced by the addition of dantrolene at different concentrations (12.5 μM, 25.0 μM, and 50.0 μM) (n = 3). Significant decreases in contractile force were observed between the low concentration groups (0 μM and 12.5 μM) versus the high concentration groups (25.0 μM and 50.0 μM) (*$P < 0.05$, Games-Howell test). Contractile forces were normalized by the force at 0 min. (c) Profiles of tetanus contractions (EPS: 15 Hz) before (0 min) and after (10 min) the addition of dantrolene (final concentration: 50.0 μM). (d) Change in contractile force of tetanus contraction by adding dantrolene at different concentrations (final concentration: 12.5 μM, 25.0 μM, and 50.0 μM). Contractile forces were normalized by the force before the addition of dantrolene (n = 3). Statistically significant differences were not observed between the groups (one-way ANOVA). Contractile forces shown in (b) and (d) were obtained from measurements of three different tissue samples.

used to treat asthma [45,46]. On the other hand, some previous studies reported that high doses of this drug may induce myocyte death in skeletal muscles, although these same studies only demonstrated the effect of clenbuterol in animal experiments using rats [47,48]. In this study, the contractile force decreased remarkably after the addition of clenbuterol at higher doses up to 100 μM. Even though EPS was applied to the muscle tissue, the contractile forces became too small to be determined quantitatively (Fig. 6a). This indicated that our muscle tissue replicated the physiological response to clenbuterol found in native muscle. On the other hand, no change in contractile force was shown with the addition of clenbuterol at lower doses (final concentration: 0.1 and 10 μM) (Fig. 6b). It has been previously reported that depending on the dose, clenbuterol enhances the contractile ability of muscle [24]. However, in this study, our muscle tissues showed no enhancement of contractile ability by treatment with lower doses (0.1 and 10 μM). Compared with the change in the 0 μM group, there were only significant decreases in the 50 μM and 100 μM clenbuterol groups (Fig. 6c). Therefore, the 3D-aligned muscle tissue only showed a decrease in contractile force at the higher dose of clenbuterol.

EPS applications at high frequency (e.g., 15 Hz) induced tetanus contractions, which continuously generated and maintained the force during the application. Our measurement system showed maintenance and reduction of contractile force in single tetanus contraction profiles. The ability to maintain the force can be used to estimate fatigue resistance of muscle tissues. Interestingly, although 10 μM dose of clenbuterol induced no change in the contractile forces (the peak of tetanus contractions) (Fig. 7), the contraction profiles before and after the addition of clenbuterol were different. Whereas the tetanus contraction was maintained before the drug treatment, the profiles after 20 min of treatments showed a higher gradient in the tetanus contraction (Fig. 7b). On the other hand, the tetanus contractions with 0.1 μM dose of clenbuterol showed similar profiles before and after the treatment. Even though the EPS was continuously applied during the single tetanus contraction, the contractile forces gradually reduced only in the case of 10 μM dose. This suggested that the specific dose of clenbuterol caused the reduction in the ability to maintain the contractile force during a tetanus contraction. Muscle fatigue is a commonly experienced phenomenon that limits athletic performance and other strenuous or prolonged activities. Since muscle fatigue induces the inability of muscles to maintain expected contractile force during sports and exercise activities, fatigue resistance is an important feature in muscle physiology. In this study, our measurement system showed that the 10 μM dose of clenbuterol caused a reduction in the fatigue resistance of our muscle tissue (Fig. 7b). Since the higher dose (50 and 100 μM) remarkably decreased contractile force, the change in the gradient of tetanus contraction was not comparable before and after the addition of clenbuterol (Fig. 7b). Therefore, to confirm the reproducibility of the reduction in the fatigue resistance, the force change in single tetanus contractions was quantitatively determined with the addition of a dose less than 10 μM (Fig. 7c) [24]. Whereas the 10 μM dose of clenbuterol caused a reduction in fatigue resistance (the ability to maintain force in a tetanus), the lower dose showed no influence on fatigue resistance. This indicated that

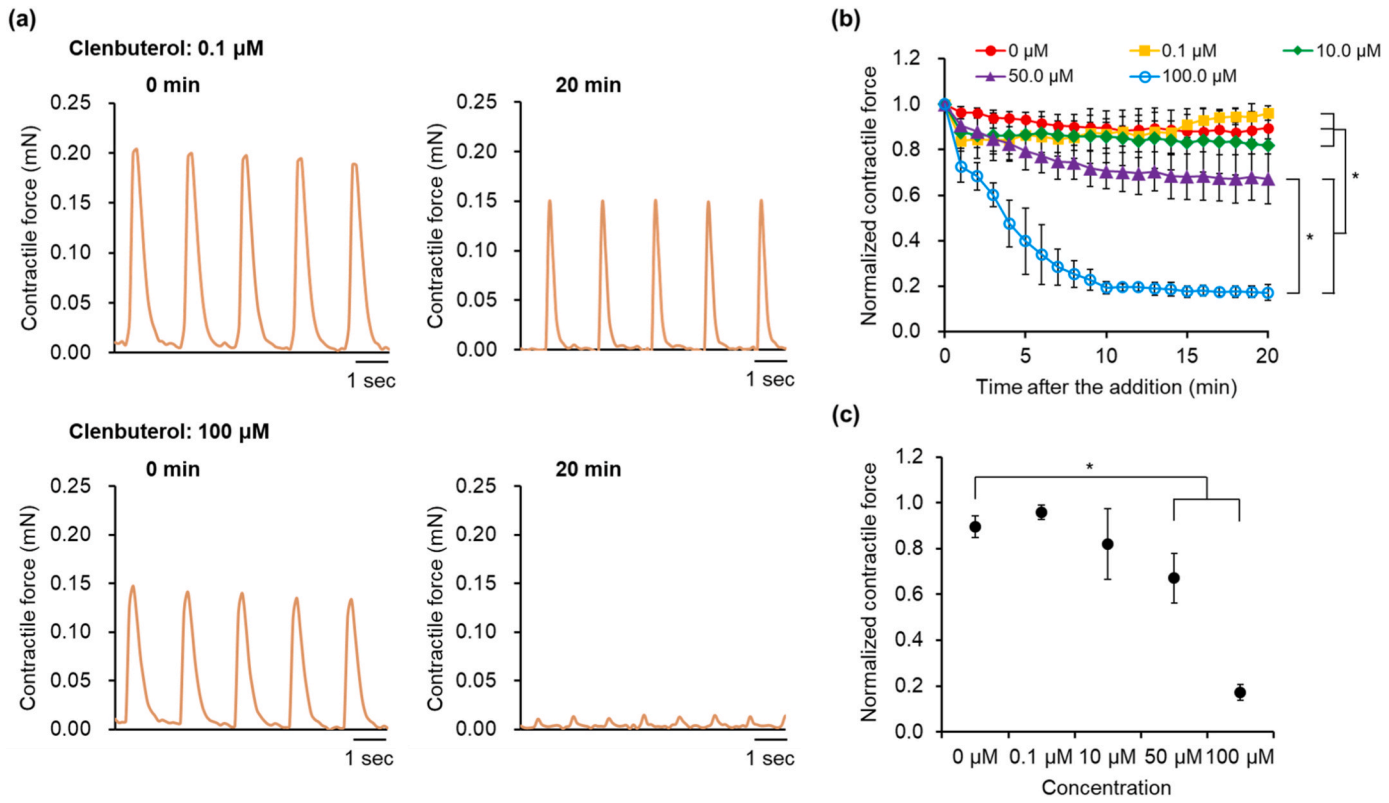

Fig. 6. Reduction in contractile force of twitch contraction by treatment with clenbuterol. (a) Twitch contractions of the 3D-aligned muscle tissue at 0 and 20 min after the addition of clenbuterol (final concentration: 0.1 μM and 100 μM). (b) Change in contractile forces generated by EPS (1 Hz) for 20 min with clenbuterol (final concentration: 0 μM, 0.1 μM, 10 μM, 50 μM, and 100 μM). Contractile forces were normalized by the force just after (0 min) the addition of clenbuterol (n = 3). The contractile force was significantly lower in the high concentration groups (50 μM and 100 μM) compared to the low concentration groups (0 μM, 0.1 μM, and 10 μM), moreover, the results of the100 μM clenbuterol group were observed to be much lower than in the 50 μM clenbuterol group (*$P < 0.05$, Games-Howell test). (c) Reduction in contractile force at 20 min after the addition of clenbuterol (final concentration: 0 μM, 0.1 μM, 10 μM, 50 μM, and 100 μM). Contractile forces were normalized by the force just after the addition of clenbuterol (n = 3). Significant decreases were observed between the no clenbuterol group (0 μM) versus the 50 μM and 100 μM clenbuterol groups (*$P < 0.05$, Dunnett's test). Contractile forces shown in (b) and (c) were obtained from measurements of three different tissue samples.

fatigue resistance in the engineered muscle tissue was reduced remarkably by the clenbuterol treatment. Importantly, this reduction in fatigue resistance was able to be observed only in tetanus, but not in twitch contractions (Fig. 6b and c). Therefore, changes in the muscle tissues affected by drugs provide different information by measuring the twitch and tetanus contractions. In this study, the real-time monitoring of tetanus contractions provided a visualization of the reduction in fatigue resistance of muscles. In addition, these results indicated that our muscle tissue model can be effectively used to replicate skeletal muscle physiology and understand the effects of various kinds of drugs in the human body.

4. Discussion

To understand muscle physiology and discover new drugs for the treatment of muscle diseases, engineered muscle tissues are urgently needed more than ever because of the advantages they will bring to research in bioscience. Although various approaches to tissue engineering have been reported to produce muscle tissues, most studies have mainly reported on the production of rodent muscle tissue models [18,19]. This has been because of the difficulty in in vitro maturation of human muscle tissue for modeling muscle physiology, compared with rodent muscle tissues. In our previous studies, we discovered that fibrin gel containing Matrigel effectively promoted in vitro maturation of human muscle tissues. In addition, the fibrin-based gel works as a platform for the attachment of the tissue to a load cell in the contractile force measurement device, which allows us to measure the contractile force of the tissue [24,33,49]. Therefore, our method using these techniques allowed us to produce human muscle tissues and then measure their contractile force. However, the previously developed method used a stepwise tissue fabrication process, which is not suitable for tissue modeling in preclinical studies. In this study, we succeeded in the simplification of the tissue engineering process. The presence of muscle satellite cells induced compaction of the fibrin-based gel, and triggered unidirectional stretching of the gel platform. The muscle satellite cells were aligned in the stretched fibrin gel, and the gel promoted maturation of the cells into contractile myofibers. In addition, the results here suggested that muscle-specific membrane structures including laminin and dystrophin were also formed in the muscle tissue. Consequently, the one-step tissue fabrication process allowed us to produce a human muscle tissue model that structurally and physiologically mimics the native muscle. Furthermore, through the one-step process, this muscle tissue is simultaneously ready for contractile force measurements in our system.

The muscle tissue model developed in this study showed physiological responses to some representative drugs and our measurement system demonstrated that the impact of the drugs caused changes in contractile forces. It is commonly understood that while both ryanodine and dantrolene interact with ryanodine receptors, their action mechanisms are different [42]. Our modeling system was effectively used to determine the similarities and differences between these two mechanisms affecting muscle contraction. The real-time monitoring clearly showed that the addition of ryanodine and dantrolene had a subtlety different influence on the engineered muscle tissue, although both drugs

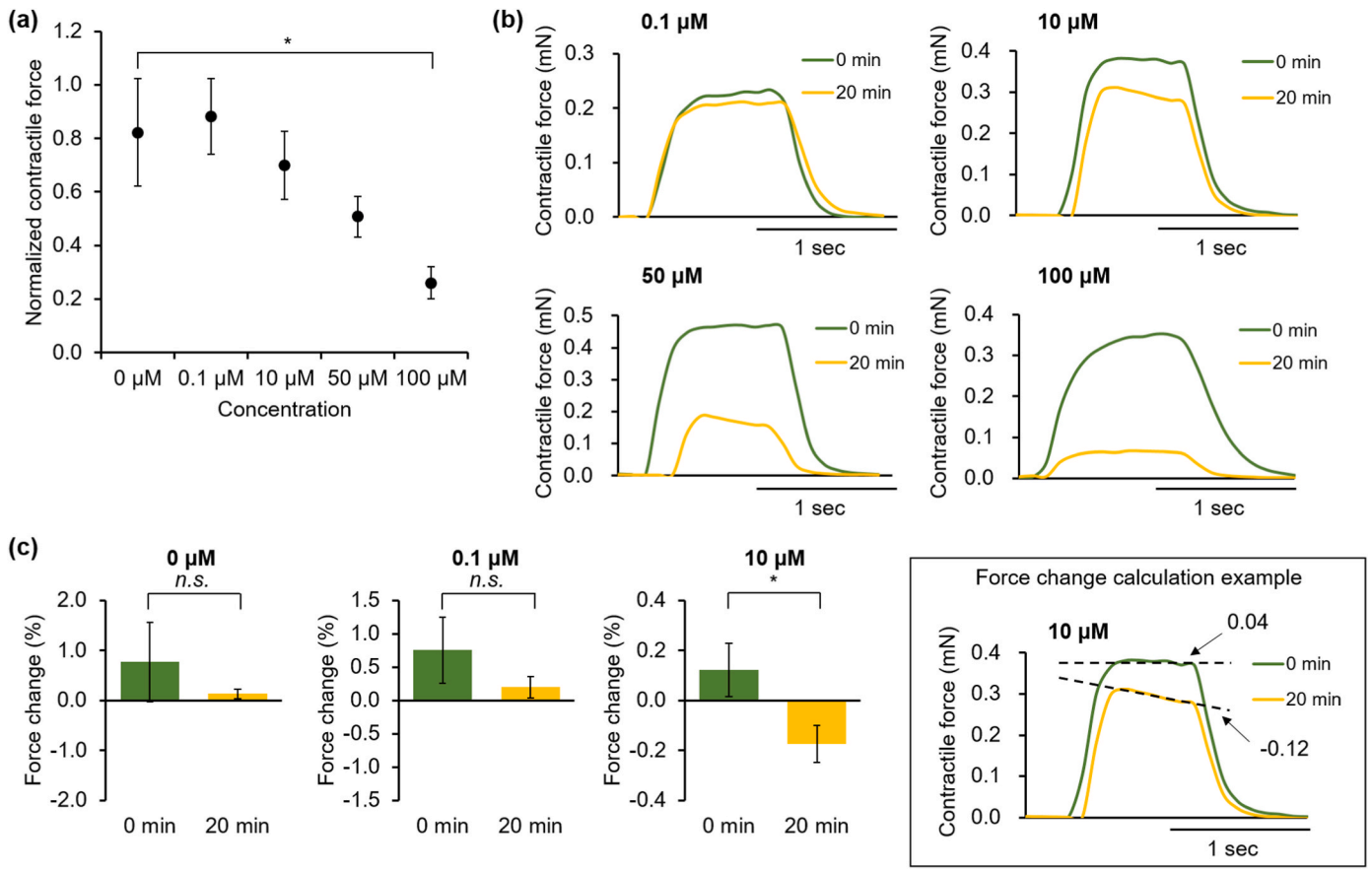

Fig. 7. Reduction of fatigue resistance (ability to maintain a tetanus contraction) in the 3D-aligned muscle tissue after treatment with clenbuterol. (a) Change in the highest contractile force in single tetanus contractions by adding clenbuterol at different concentrations (final concentration: 0 μM, 0.1 μM, 10 μM, 50 μM, and 100 μM). Contractile forces were normalized by the force before the addition of clenbuterol (n = 3). A significant decrease was observed between the 0 μM clenbuterol group and the 100 μM clenbuterol group (*$P < 0.05$, Dunnett's test). (b) Profiles of a tetanus contraction at 0 and 20 min after adding clenbuterol (final concentration: 0.1 μM, 10 μM, 50 μM, and 100 μM). EPS (frequency: 15 Hz) was applied to produce tetanus contractions in the same tissue samples at 0 and 20 min after adding clenbuterol. (c) Force change in single tetanus contractions (the ability to maintain a tetanus contraction) with clenbuterol at different concentrations (0 μM, 0.1 μM, and 10 μM) (n = 3). Only in the 10 μM clenbuterol group, there was a significant difference between before and after the addition of clenbuterol (*$P < 0.05$, Student's t-test). Contractile forces shown in (a) and (c) were obtained from measurements in three different tissue samples.

induced a reduction in contractile force (Figs. 4 and 5). Furthermore, our tissue model showed a reduction in fatigue resistance by adding clenbuterol at a specific concentration (10 μM). Whereas this delicate change was observed only by monitoring the profile of tetanus contractions, our measurement system reproducibility showed a reduction in fatigue resistance (Fig. 7). Therefore, these results indicate that this engineered human muscle tissue is highly reliable as a tissue model for clinically relevant in vitro studies in muscle physiology and drug discovery for muscle diseases.

Although the responses shown in this study were similar to those of human muscle tissues developed in some previous studies, the addition of low concentrations of clenbuterol did not enhance the contractile force [16]. This probably indicates that the muscle tissue produced in this study had some limitations in replicating mechanisms of native skeletal muscle. For example, the ratio of cell/ECM in the engineered muscle tissue was likely lower than that in native muscle, which is closely related with muscle tissue stiffness. In addition, some, but not all nuclei were located along the periphery of myofibers. In native muscle, all nuclei are typically located between a myofiber and a membrane to efficiently produce a contractile force. Therefore, the nuclei position possibly caused the difference found in this study. More importantly, the contractile force generated by this muscle tissue was much lower than that of native muscle. From these viewpoints, the functionality of our muscle tissue needs to be further matured to more closely mimic native muscle in the future. On the other hand, various types of currently developed tissue models, including ours are sufficiently useful for drug discovery research, depending on the characteristics of tissue models and the purpose of each preclinical study. This study demonstrated a simpler method for creating muscle tissue models and evaluating the effects of drugs on muscle. Therefore, we believe that this tissue engineering method will become an option for producing preclinical muscle tissue models in future studies.

5. Conclusion

In this study, the one-step tissue fabrication approach allowed us to produce contractile human muscle tissue with a biomimetic-aligned structure. The cell-induced gel compaction triggered the unidirectional stretching of the fibrin-based gel and the aligned orientation of the myofibers in the gel. The gel environment also promoted the maturation of the aligned cells and subsequently the muscle tissues produced twitch and tetanus contractions according to electrical stimulation conditions. In addition, since our muscle tissues were fabricated with adaptors specifically designed for our measurement device, additional steps were not necessary for the contractile force measurement. Our tissue model system allowed us to estimate quantitatively contractile forces of human muscle tissues induced by electrical and chemical stimulations. The changes in contractile force in some of the drug tests were successfully measured quantitatively in real-time. In addition, the reduction in fatigue resistance induced by a specific dose of clenbuterol was

reproducibly observed in our measurement system. Both the physiological responses to the drugs shown in this study indicate that our engineered muscle tissue fabricated in one step can be highly reliable as a preclinical human tissue model for in vitro studies in muscle physiology and drug discovery.

CRediT authorship contribution statement

Azumi Yoshida: Writing – original draft, Visualization, Validation, Methodology, Investigation, Data curation. **Kazuki Baba:** Methodology, Investigation, Data curation. **Hironobu Takahashi:** Writing – original draft, Validation, Supervision, Methodology, Funding acquisition, Data curation, Conceptualization. **Kenichi Nagese:** Writing – review & editing, Resources. **Tatsuya Shimizu:** Writing – review & editing, Validation, Supervision.

Declaration of competing interest

The authors declare the following financial interests/personal relationships which may be considered as potential competing interests. Tatsuya Shimizu is a stakeholder in CellSeed Inc. Tokyo Women's Medical University receives research funds from CellSeed Inc, and NIHON KOHDEN Corporation.

Acknowledgements

We gratefully acknowledge Mr. Yuto Hinata (NIHON KOHDEN Corporation) for his technical assistance. We also thank Mr. Allan Nisbet for his useful comments and editorial assistance. This work was supported by JSPS KAKENHI Grant Number JP21KK0199.

Appendix A. Supplementary data

Supplementary data to this article can be found online at https://doi.org/10.1016/j.mtbio.2025.101456.

Data availability

Data will be made available on request.

References

[1] J.A. DiMasi, L. Feldman, A. Seckler, A. Wilson, Trends in risks associated with new drug development: success rates for investigational drugs, Clinical Pharmacology & Therapeutics 87 (3) (2010) 272–277.
[2] M. Hay, D.W. Thomas, J.L. Craighead, C. Economides, J. Rosenthal, Clinical development success rates for investigational drugs, Nat. Biotechnol. 32 (1) (2014) 40–51.
[3] P.D. Thompson, P.M. Clarkson, R.S. Rosenson, An assessment of statin safety by muscle experts, Am. J. Cardiol. 97 (8) (2006) S69–S76. Supplement 1.
[4] B. Fine, G. Vunjak-Novakovic, Shortcomings of animal models and the rise of engineered human cardiac tissue, ACS Biomater. Sci. Eng. 3 (9) (2017) 1884–1897.
[5] M. Mills, M.K. Estes, Physiologically relevant human tissue models for infectious diseases, Drug Discov. Today 21 (9) (2016) 1540–1552.
[6] S.N. Bhatia, D.E. Ingber, Microfluidic organs-on-chips, Nat. Biotechnol. 32 (8) (2014) 760–772.
[7] K.-H. Nam, A.S.T. Smith, S. Lone, S. Kwon, D.-H. Kim, Biomimetic 3D tissue models for advanced high-throughput drug screening, J. Lab. Autom. 20 (3) (2015) 201–215.
[8] A. Mathur, Z. Ma, P. Loskill, S. Jeeawoody, K.E. Healy, In vitro cardiac tissue models: current status and future prospects, Adv. Drug Deliv. Rev. 96 (2016) 203–213.
[9] D. Huh, B.D. Matthews, A. Mammoto, M. Montoya-Zavala, H.Y. Hsin, D.E. Ingber, Reconstituting organ-level lung functions on a chip, Science 328 (5986) (2010) 1662–1668.
[10] M. Juhas, G.C. Engelmayr Jr., A.N. Fontanella, G.M. Palmer, N. Bursac, Biomimetic engineered muscle with capacity for vascular integration and functional maturation in vivo, Proc Natl Acad Sci U S A 111 (15) (2014) 5508–5513.
[11] M.H. Mohammadi, R. Obregón, S. Ahadian, J. Ramón-Azcón, M. Radisic, Engineered muscle tissues for disease modeling and drug screening applications, Curr. Pharmaceut. Des. 23 (20) (2017) 2991–3004.
[12] A.S.T. Smith, J. Davis, G. Lee, D.L. Mack, D.H. Kim, Muscular dystrophy in a dish: engineered human skeletal muscle mimetics for disease modeling and drug discovery, Drug Discov. Today 21 (9) (2016) 1387–1398.
[13] J. Wang, A. Khodabukus, L. Rao, K. Vandusen, N. Abutaleb, N. Bursac, Engineered skeletal muscles for disease modeling and drug discovery, Biomaterials 221 (2019) 119416.
[14] L. Janssen, N.A.E. Allard, C.G.J. Saris, J. Keijer, M.T.E. Hopman, S. Timmers, Muscle toxicity of drugs: when drugs turn physiology into pathophysiology, Physiol. Rev. 100 (2) (2020) 633–672.
[15] C.D. Furberg, B. Pitt, Withdrawal of cerivastatin from the world market, Trials 2 (5) (2001) 205.
[16] L. Madden, M. Juhas, W.E. Kraus, G.A. Truskey, N. Bursac, Bioengineered human myobundles mimic clinical responses of skeletal muscle to drugs, Elife 4 (2015).
[17] A. Khodabukus, N. Prabhu, J. Wang, N. Bursac, In vitro tissue-engineered skeletal muscle models for studying muscle physiology and disease, Adv Healthc Mater 7 (15) (2018) e1701498.
[18] H. Vandenburgh, J. Shansky, F. Benesch-Lee, V. Barbata, J. Reid, L. Thorrez, R. Valentini, G. Crawford, Drug-screening platform based on the contractility of tissue-engineered muscle, Muscle Nerve 37 (4) (2008) 438–447.
[19] A. García-Lizarribar, A. Villasante, J.A. Lopez-Martin, M. Flandez, M.C. Soler-Vázquez, D. Serra, L. Herrero, A. Sagrera, A. Efeyan, J. Samitier, 3D bioprinted functional skeletal muscle models have potential applications for studies of muscle wasting in cancer cachexia, Biomater. Adv. 150 (2023) 213426.
[20] W. Bian, N. Bursac, Engineered skeletal muscle tissue networks with controllable architecture, Biomaterials 30 (7) (2009) 1401–1412.
[21] L. Rao, Y. Qian, A. Khodabukus, T. Ribar, N. Bursac, Engineering human pluripotent stem cells into a functional skeletal muscle tissue, Nat. Commun. 9 (1) (2018) 126.
[22] A. Khodabukus, L. Madden, N.K. Prabhu, T.R. Koves, C.P. Jackman, D.M. Muoio, N. Bursac, Electrical stimulation increases hypertrophy and metabolic flux in tissue-engineered human skeletal muscle, Biomaterials 198 (2019) 259–269.
[23] H. Takahashi, T. Shimizu, T. Okano, Engineered human contractile myofiber sheets as a platform for studies of skeletal muscle physiology, Sci. Rep. 8 (1) (2018) 13932.
[24] H. Takahashi, H. Wakayama, K. Nagase, T. Shimizu, Engineered human muscle tissue from multilayered aligned myofiber sheets for studies of muscle physiology and predicting drug response, Small Methods 7 (2) (2023) 2200849.
[25] J.H. Kim, Y.J. Seol, I.K. Ko, H.W. Kang, Y.K. Lee, J.J. Yoo, A. Atala, S.J. Lee, 3D bioprinted human skeletal muscle constructs for muscle function restoration, Sci. Rep. 8 (1) (2018) 12307.
[26] H. Takahashi, T. Okano, Thermally-triggered fabrication of cell sheets for tissue engineering and regenerative medicine, Adv. Drug Deliv. Rev. 138 (2019) 276–292.
[27] J. Kobayashi, A. Kikuchi, T. Aoyagi, T. Okano, Cell sheet tissue engineering: cell sheet preparation, harvesting/manipulation, and transplantation, J. Biomed. Mater. Res. 107 (5) (2019) 955–967.
[28] H. Takahashi, M. Nakayama, T. Shimizu, M. Yamato, T. Okano, Anisotropic cell sheets for constructing three-dimensional tissue with well-organized cell orientation, Biomaterials 32 (34) (2011) 8830–8838.
[29] H. Takahashi, M. Nakayama, K. Itoga, M. Yamato, T. Okano, Micropatterned thermoresponsive polymer brush surfaces for fabricating cell sheets with well-controlled orientational structures, Biomacromolecules 12 (5) (2011) 1414–1418.
[30] H. Takahashi, F. Oikawa, N. Takeda, T. Shimizu, Contraction control of aligned myofiber sheet tissue by parallel oriented induced pluripotent stem cell-derived neurons, Tissue Eng. 28 (15–16) (2022) 661–671.
[31] H. Takahashi, A. Yoshida, B. Gao, K. Yamanaka, T. Shimizu, Harvest of quality-controlled bovine myogenic cells and biomimetic bovine muscle tissue engineering for sustainable meat production, Biomaterials 287 (2022) 121649.
[32] H. Takahashi, K. Ishiyama, N. Takeda, T. Shimizu, Nutrient rescue of early maturing and deteriorating satellite cell-derived engineered muscle tissue, Tissue Eng. 29 (23–24) (2023) 633–644.
[33] Y. Hinata, Y. Kagawa, H. Kubo, E. Kato, A. Baba, D. Sasaki, K. Matsuura, K. Sawada, T. Shimizu, Importance of beating rate control for the analysis of drug effects on contractility in human induced pluripotent stem cell-derived cardiomyocytes, J. Pharmacol. Toxicol. Methods 118 (2022) 107228.
[34] M.D. Stevenson, A.L. Sieminski, C.M. McLeod, F.J. Byfield, V.H. Barocas, K. J. Gooch, Pericellular conditions regulate extent of cell-mediated compaction of collagen gels, Biophys. J. 99 (2010) 19–28.
[35] U. Doha, O. Aydin, M.S.H. Joy, B. Emon, W. Drennan, M.T.A. Saif, Disorder to order transition in cell-ECM systems mediated by cell-cell collective interactions, Acta Biomater. 154 (2022) 290–301.
[36] A.E.X. Brown, R.I. Litvinov, D.E. Discher, P.K. Purohit, J.W. Weisel, Multiscale mechanics of fibrin polymer: gel stretching with protein unfolding and loss of water, Science 325 (5941) (2009) 741–744.
[37] R.I. Litvinov, J.W. Weisel, Fibrin mechanical properties and their structural origins, Matrix Biol. 60–61 (2017) 110–123.
[38] T. Uchimura, J. Otomo, M. Sato, H. Sakurai, A human iPS cell myogenic differentiation system permitting high-throughput drug screening, Stem Cell Res. 25 (2017) 98–106.
[39] N. Jiwlawat, E. Lynch, J. Jeffrey, J.M. Van Dyke, M. Suzuki, Current progress and challenges for skeletal muscle differentiation from human pluripotent stem cells using transgene-free approaches, Stem Cells Int 2018 (2018) 6241681.
[40] F. Sakai-Takemura, A. Narita, S. Masuda, T. Wakamatsu, N. Watanabe, T. Nishiyama, K. Nogami, M. Blanc, S. Takeda, Y. Miyagoe-Suzuki, Premyogenic progenitors derived from human pluripotent stem cells expand in floating culture

and differentiate into transplantable myogenic progenitors, Sci. Rep. 8 (1) (2018) 6555.
[41] P.M. Rodríguez Cruz, J. Cossins, D. Beeson, A. Vincent, The neuromusclular junction in health and disease: molecular mechanisms governing synaptic formation and homeostasis, Front. Mol. Neurosci. 13 (2020) 610964.
[42] B.R. Fruen, J.R. Mickelson, C.F. Louis, Dantrolene inhibition of sarcoplasmic reticulum Ca2+Release by direct and specific action at skeletal muscle ryanodine receptors, J. Biol. Chem. 272 (43) (1997) 26965–26971.
[43] G. Santulli, D.R. Lewis, A.R. Marks, Physiology and pathophysiology of excitation-contraction coupling: the functional role of ryanodine receptor, J. Muscle Res. Cell Motil. 38 (1) (2017) 37–45.
[44] T. Krause, M.U. Gerbershagen, M. Fiege, R. Weißhorn, F. Wappler, Dantrolene – a review of its pharmacology, therapeutic use and new developments, Anaesthesia 59 (4) (2004) 364–373.
[45] T. Kita, M. Fujimura, H. Ogawa, Y. Nakatsumi, S. Nomura, Y. Ishiura, S. Myou, S. Nakao, Antitussive effects of the leukotriene receptor antagonist montelukast in patients with cough variant asthma and atopic cough, Allergol. Int. 59 (2) (2010) 185–192.
[46] B. Waldeck, β-Adrenoceptor agonists and asthma—100 years of development, Eur. J. Pharmacol. 445 (1) (2002) 1–12.
[47] J.G. Burniston, Y. Ng, W.A. Clark, J. Colyer, L.-B. Tan, D.F. Goldspink, Myotoxic effects of clenbuterol in the rat heart and soleus muscle, J. Appl. Physiol. 93 (5) (2002) 1824–1832.
[48] J.G. Burniston, W.A. Clark, L.B. Tan, D.F. Goldspink, Dose-dependent separation of the hypertrophic and myotoxic effects of the beta(2)-adrenergic receptor agonist clenbuterol in rat striated muscles, Muscle Nerve 33 (5) (2006) 655–663.
[49] D. Sasaki, K. Matsuura, H. Seta, Y. Haraguchi, T. Okano, T. Shimizu, Contractile force measurement of human induced pluripotent stem cell-derived cardiac cell sheet-tissue, PLoS One 13 (5) (2018) e0198026.